Internal short-circuits faults localization in transformer windings using FRA and natural frequencies deviation patterns

V.S. Larin
All-Russian Electrotechnical Institute (FGUP VEI)
Russian Federation

SUMMARY

Frequency-response analysis (FRA) is now widely used for condition assessment of power transformers and shunt reactors and detection of internal faults.

Currently an approach of comparison of two FRA measurements using correlation analysis is widely used. Despite the simplicity of this approach, its application does not provide ability for the interpretation of the type of defect and its location because, in fact, it is based on comparison of the integral values (the coefficients of pair correlation) without considering the specifics of the object of measurement.

Frequency response of certain winding measured by terminal-to-terminal scheme contains the set of resonant and antiresonant frequencies having different nature. Some of resonant frequencies correspond to winding natural frequencies. These frequencies are fundamental characteristics of each winding and are mainly affected by electrical length of the winding, physical parameters of winding longitudinal insulation (e.g. dielectric permittivity of turn-to-turn insulation), arrangement and electromagnetic coupling of different parts of the winding, constraints on spatial voltage distribution inside the winding (connection between winding parts, connection of winding terminals to earth etc.).

The changes in winding natural frequencies are connected with major winding faults and have different patterns depending on type of faults or its location. These patterns can be used for the purpose of FRA interpretation.

This report describes the detection and localization of internal short-circuit faults using FRA and application of natural frequencies deviation patterns.

Report presents results obtained from white-box and physical models of disc-type windings showing the typical patterns of natural frequencies deviation corresponding to different location of turn-to-turn and disc-to-disc faults. An approach is presented allowing detection and quantitative evaluation of relative position of internal short-circuit faults inside the disc-type windings.

KEYWORDS

Power transformers, internal short-circuit faults, winding condition assessment, frequency responses, Frequency Response Analysis, FRA-measurement interpretation.

1. INTRODUCTION

Frequency response analysis (FRA) is increasingly used to assess the mechanical condition of windings of power transformers and shunt reactors during their transportation and operation.

Interpretation of FRA measurement results is usually performed by comparison between the measured frequency responses using correlation analysis and various indices [1], showing a difference of frequency responses in a wide frequency range.

The approach based on pair correlation coefficients are reflected in the standard DL/T 911-2004 [2] and is implemented in many commercial FRA instruments.

Despite its simplicity, this approach, being based on the integral indicators, does not allow to take into account the specifics of object under measurement and interpret a type and location of the faults. The standard DL/T 911-2004 strictly set the three frequency ranges (0 – 100 kHz, 100 – 600 kHz and 600 – 1000 kHz) without regard to the type of winding and the typical values of its natural frequencies. Changes of the frequency responses in the first frequency range are used as an indicator of severe damage of the windings, while the changes in the second frequency range with equal correlation coefficient is classified as less serious winding damage.

It is obvious that usage of fixed frequency bands is quite conditional, reflects some particular cases and has various levels of applicability depending on the type of windings. For example, continuous disc-type high-voltage windings have a first natural frequency typically of the order of 10-20 kHz, thus the first 5 … 10 natural frequencies will be located in the first frequency band (0 – 100 kHz). The first natural frequency of helical and multilayer low-voltage windings can be of the order of 200-300 kHz, so the first natural frequency will be in the second frequency range (100 – 600 kHz).

It was shown previously in [3] that qualitatively different manner of the FRA interpretation can be made on the basis of the analysis of the design features of the object of measurement and applied types of windings based on the analysis of the natural frequencies of these windings.

The frequency response of individual winding, measured by end-to-end schemes, contains the set of resonant and anti-resonant frequencies with different nature. The individual resonant frequencies correspond to the natural frequencies of winding oscillations, which are their fundamental characteristics. These frequencies are primarily dependent on the electrical length of the winding, the physical parameters of longitudinal winding insulation (e.g., dielectric constant of longitudinal insulation), the location and the electromagnetic coupling of the individual parts of the winding, restrictions on the spatial voltage distribution within the winding (the connection between the winding parts, the connection of winding terminals to earth).

Changes of winding natural frequencies are usually associated with serious winding faults and have different pattern depending on the type of faults and its location.

This report presents an improvement of approach to the FRA interpretation using the patterns of winding natural frequencies deviations and its application in case of winding internal short-circuit faults (turn-to-turn and disc-to-disc) in the power transformers and reactors.

In view of transformer condition assessment the solution of two main tasks is of interest, namely:
1) Detection of internal short-circuit fault in the windings.
2) Localization of short-circuit fault in the winding.

With respect to transformer condition assessment in operation the second task is rather optional, since the presence of internal short-circuit fault significantly limits further transformer utilization. However, this task is demanded in the case of subsequent disassembling and inspection of the transformer in order to identify internal faults and causes of damage and assess the transformer repairability.

The first task can be solved by using traditional methods of diagnosis such as measurement of no-load losses, voltage ratio and winding resistance, but these methods cannot solve the second task.

The solution of first task, i.e. determining the presence of internal short-circuit fault, can be performed using the FRA by comparing frequency responses before and after damage, and by comparing frequency responses between the phases of the transformer.

Recently the works on development of the FRA interpretation and identification of winding internal short-circuit faults are well under way. For instance, the reference [4] presents the results of measurements on a physical model of the transformer with multilayer cylindrical windings by varying the inter-winding fault locations and resistance of the short-circuit jumper. In reference [5] the results of computer modeling of short-circuit faults in multilayer cylindrical winding and the dependences of

2

deviations of frequency and amplitude the winding impedance maxima depending on the location of faults are presented. In reference [6] the conclusion about the possibility of assessing the place of disc-to-disc short-circuit fault by constructing the amplitude-phase frequency response (Nyquist plot) was made based on measurements on the physical model. Various approaches of internal faults interpretation were proposed such as approach based on transfer function analysis [7] and approach based on frequency response plotting in polar coordinates [8].

In reference [9] the results of measurement of the HV-to-LV and LV-to-HV transfer functions and the impedance of multilayer cylindrical winding with regards to short circuit of individual layers were presented and the symmetry of the variation of winding impedance depending on internal short-circuit fault location regarding winding middle were noted.

This report shows the results of studies conducted on continuous disc windings to identify the possibility of solutions of the abovementioned second task, i.e. approximate location of winding internal short-circuit faults using the FRA.

2. DETERMINATION OF WINDING NATURAL FREQUENCIES

The approach under development is based on the analysis of changes of natural frequencies of transformer windings. To identify the natural frequencies an approach [3, 10] can be used which is based on the comparison of the winding frequency responses measured with open and shorted secondary windings as well as analysis of winding active admittance calculated from amplitude and phase of frequency responses.

An idea of this approach is that the spatial distribution of winding current at first natural frequencies has nodes in which the current changes direction. As result the currents in adjacent winding sections near these nodes have the opposite direction. The EMF induced in the turns of the secondary winding are mutually compensated, and the magnetic flux generated by the primary winding penetrates the magnetic core, without encountering reaction from the secondary winding.

Thus, the short circuit of secondary winding has practically no effect on the admittance of primary winding at the frequencies corresponding to natural frequencies of the considered primary winding and has no influence on values of these natural frequencies.

However, at frequencies much lower than the first winding natural frequency the condition of secondary winding, its short-circuiting, has an influence on the penetration of magnetic flux in the magnetic circuit and return path of magnetic flux, and therefore leads to a significant changes in the admittance of considered primary winding and resonant frequencies related to interaction between windings (figure 1). This rule applies both for outermost HV windings and innermost LV windings.
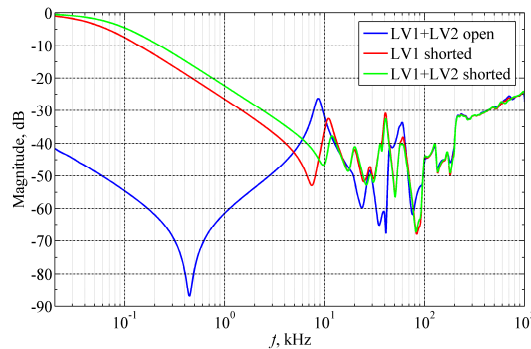

Figure 1 – Frequency response of primary winding measured with open and shorted splitted secondary windings (LV1 and LV2)

The algorithm for determining the winding natural frequencies [3, 10] contains the following main steps:

1. Approximate evaluation of winding admittance based on measured frequency responses corresponding to open-circuited and short-circuited secondary winding

$$\overline{Y}_{12} = \left(\frac{1}{Z_c} + j\omega C_s\right)\frac{\overline{U}_2}{\overline{U}_1 - \overline{U}_2} \approx \left[Z_c\left(\frac{1}{A\angle\varphi} - 1\right)\right]^{-1},\tag{1}$$

3

where $\overline{U}_1$ and $\overline{U}_2$ – input and output voltage; $A = \left| \overline{U}_2 / \overline{U}_1 \right|$; $\varphi = \angle(\overline{U}_2, \overline{U}_1)$; Z_c – matching impedance of response measurement channel; C_s – capacitance to earth at connection point of response measurement channel (capacitance of bushing, capacitance of leads connecting winding end to bushing and leads between windings as well as capacitance of measurement cables and connecting wires).

2. Approximate evaluation of winding active admittance $\overline{G}_{12}$ as real part of $\overline{Y}_{12}$.

3. Determination of resonant frequencies, which corresponds to maxima of $\overline{G}_{12}$ at open-circuit and short-circuit condition of secondary winding.

4. Identification of natural frequencies as resonant frequencies at which there is an agreement between frequency responses (active admittances) corresponding to open and shorted secondary winding.

It should be noted that the presence of the parasitic capacitance Cs causes an error of evaluation of admittance and its real part based on the results of FRA measurements which is increasing with the growth of frequency. It can be observed in high frequency range, for example, by means of abnormal increase of active admittance (figure 2,*a*), obtained from the expression (1). However, in practical cases, this error begins to affect at the frequencies closer to 1 MHz, and generally does not preclude from determination of winding natural frequencies of power transformers and shunt reactors in the frequency range up to several hundred kHz.
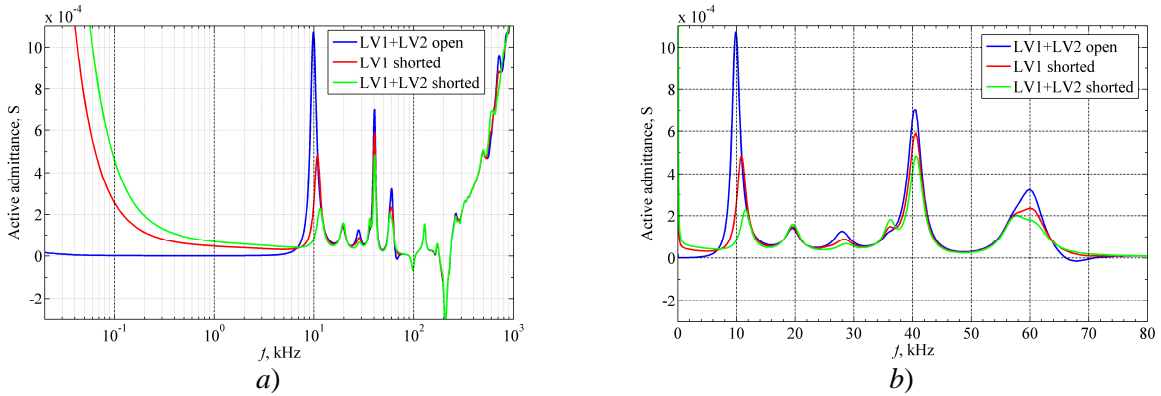

a)   *b)*

Figure 2 – Active admittance of primary winding with open and shorted splitted secondary winding: logarithmic scale (*a*) and zoomed linear scale (*b*)

3. DETERMINATION OF WINDING SHORT-CIRCUIT FAULTS

Reference [3] presents the results of studies of frequency response deviations in the presence of turn-to-turn and disc-to-disc short-circuit faults performed on a real-scale physical model of continuous dis-type winding.

Typical experimentally obtained dependences of the deviations *df* of the first five natural frequencies in the case of disc-to-disc short-circuit faults are shown in figure 3 (similar results were also obtained by modeling with usage of white-box models), where *L* is relative electrical distance from the winding start to a midpoint of a winding section affected by the short circuit.
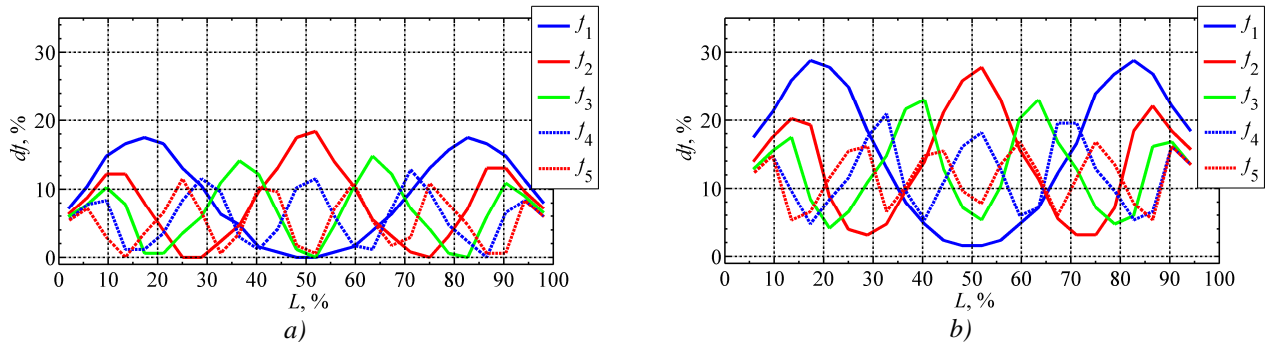

a)   *b)*

Figure 3 – Winding natural frequency deviation in case of short-circuiting of two (*a*) and six (*b*) adjacent discs [3]

4

As it can be seen from figure 3, in case of internal short-circuit faults there are the certain patterns of winding natural frequencies deviations, depending on the location of the short-circuit fault. These patterns are almost symmetrical when considered winding is symmetrical about its middle.

The obtained dependences can be explained on the basis of the spatial voltage distribution along the windings at one of its natural frequencies.

The spatial voltage distribution and considered natural frequency do not change significantly when short-circuit occurs between winding points having approximately equal values of potential. For example, when the short circuit occurs in the middle of winding, the changes of odd natural frequencies will be negligible (figure 3), because maximum of spatial voltage distribution at odd natural frequencies takes place in the middle of winding. And vice versa, the short circuit of winding section near the nodes of the spatial voltage distribution at certain natural frequency leads to a significant change of this particular natural frequency. So, the short circuit at the winding start and end leads to increase of all natural frequencies, but short circuit at winding middle leads to increase in the second, fourth and so on natural frequencies.

Considered essence of the natural frequencies can be used for interpretation of FRA measurements and solving of the two above-mentioned practical tasks of diagnostics related to short-circuit faults. In general, the internal short circuit leads to reduction of the electrical length of the winding, and therefore the winding natural frequencies shall either increase or remain almost unchanged (if the short-circuit fault occurs near the maximum of spatial voltage distribution at certain natural frequencies). This important property can be used as one of the main sign of the internal short-circuit fault in the winding.

In case of winding placed on the magnetic core another sign of the internal short-circuit fault is a significant increase of first antiresonance frequency in frequency response corresponding to open secondary winding. The first antiresonance frequency is typically of the order of hundreds of Hz to few kHz, but in the case of the short-circuit faults it may increase significantly depending on the scale of the short-circuit faults.

It should be noted that the increase of first antiresonance frequency is not a sign of the presence of a short circuit exactly in the winding under measurement, because the increase occurs in the frequency responses of all windings of the same core (figure 4).
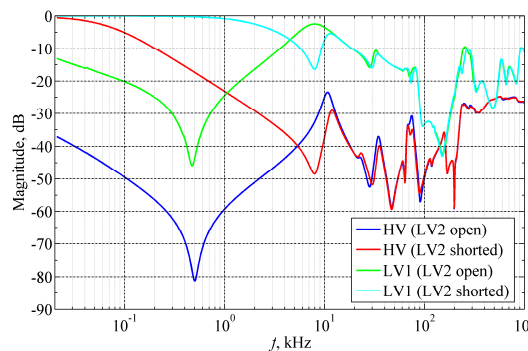

Figure 4 – Frequency response of transformer with splitted LV winding

Thus, the signs of internal short-circuit faults can be:
1) Significant increase of the first antiresonance frequency (up to several times, necessary but not sufficient condition);
2) Increase of the first natural frequencies of the winding (sufficient condition).

4. LOCALIZATION OF INTERNAL SHORT-CIRCUIT FAULTS

In order to reveal the possibility of localization of internal short circuits in the windings the studies were conducted using white-box modelling and experimental measurements on physical models:
- Model No. 1 (figure 5,a) which contains a continuous disc winding without magnetic system; the winding consists of 52 discs, the total number of turns of windings 516; the dimensions of winding correspond approximately to the high-voltage winding of transformers having voltage classes of 110 kV and above;

- Model No. 2 (figure 5,b) which contains a magnetic system with two core legs, each having an identical continuous disc winding containing 54 discs with 7 turns in each; the average diameter and height of the windings are approximately 430 mm and 900 mm correspondingly.
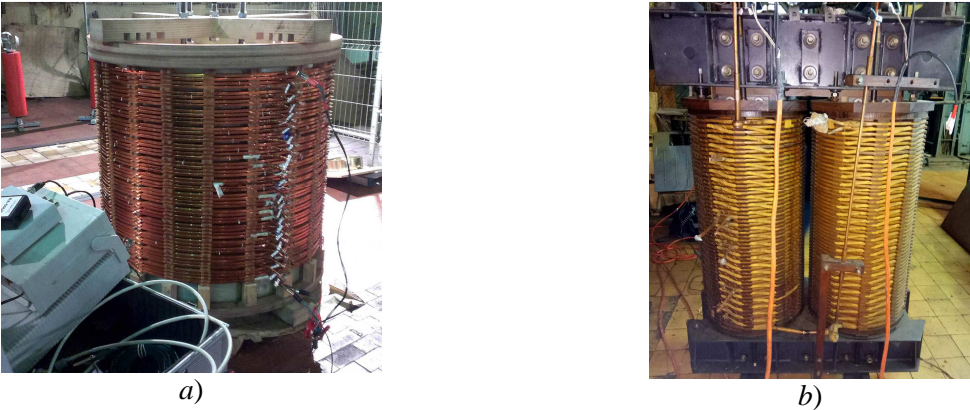

a)   *b)*

Figure 5 – Models No. 1 (*a*) and No. 2 (*b*)

The main results of experimental studies on model No. 1 are given in [3]. In this report new results of analysis of measurement are presented.

The deviations of first three natural frequencies shown in figure 3 can be represented in the form of the pattern on the radar chart.

It can be shown that usage of more than three natural frequencies can increase the accuracy of determining the location of internal short circuit. But for simplicity the description of the approach using the first three natural frequencies is given below.

To plot the pattern on the radar chart it is necessary to use relative values of deviation df_1', df_2' and df_3' which can be obtained from dividing of the estimated values of natural frequencies deviations df_1, df_2 and df_3 to the base values.

In general, the maximum value of deviation $df_{i.max}$ within the entire length of the winding (see figure 3) for i-th natural frequency can be used as base value for the i-th natural frequencies, but this value is usually unknown. Alternatively, base value df_{base} for constructing a radar chart can be taken as maximum of the current values of natural frequencies deviations: $df_{base} = \max(df_1, df_2, df_3)$.

Figure 6 shows typical patterns in the form of triangles of natural frequencies deviations for the three cases of short circuit of the two discs, located at a relative distance $L = 21,2, 36,5$ and $48,1\%$.

Figure 7 shows an alternative presentation of patterns in the form of points corresponding to the centroids (centres of mass) of the triangles of the natural frequencies deviations.
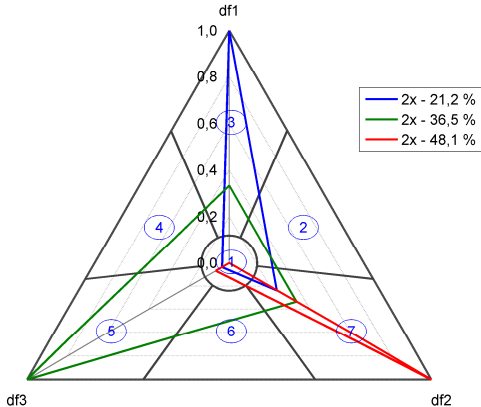

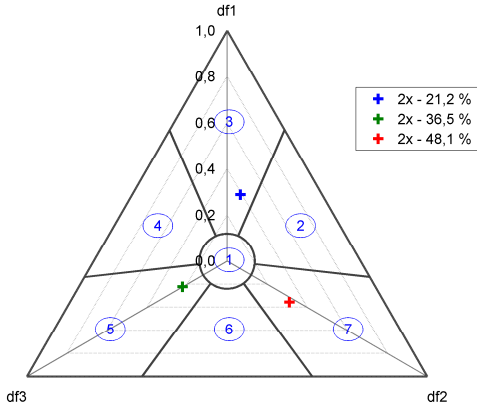Figure 6 – Triangles of natural frequencies deviations

Figure 7 – Centroids of triangles of natural frequencies deviations

The position of the center of mass of the triangle of natural frequencies deviations in the Cartesian coordinates can be calculated as:

$$x_0 = \frac{df_2' - df_3'}{2\sqrt{3}}; \quad y_0 = \frac{2df_1' - df_2' - df_3'}{6}.$$

Using the representation of the centers of mass of triangles, the measurement results shown in figure 3 will take the form shown in figure 8.
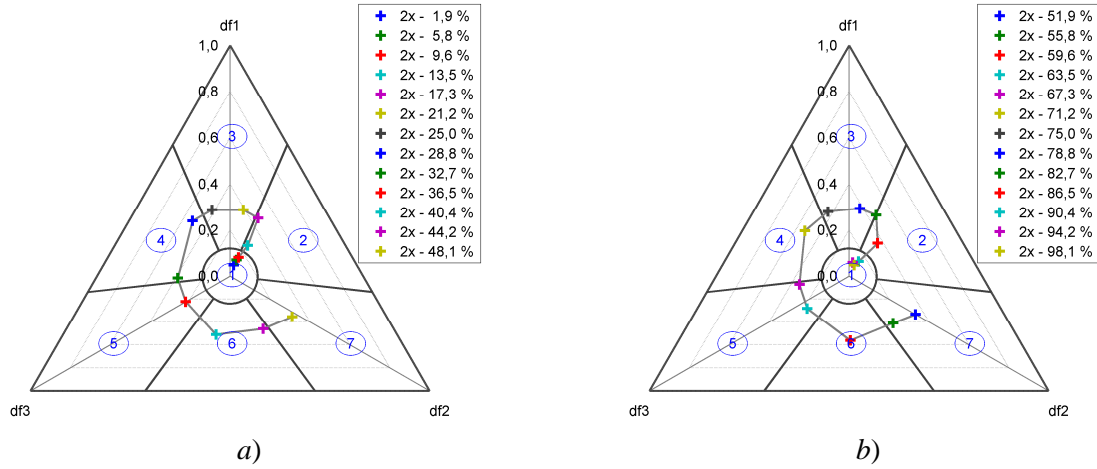

a)

b)

Figure 8 – Centroids of triangles of natural frequencies deviation in case of short circuit of two discs located at $L = 0 \div 50\%$ (*a*) and $L = 50 \div 100\%$ (*b*)

From figure 8 it can be seen that the centroids of triangles are rotated in counter-clockwise direction on a spiral path from region No. 1 to region No. 7 when short-circuit location is moved from winding start to winding middle. Further movement of short-circuit location in the direction to the winding end leads to reverse rotation of centroids from region No. 7 to region No. 1.

Thus the coordinates of the centroids can be conveniently represented in polar coordinates:

$$r_0 = \sqrt{x_0^2 + y_0^2}; \quad \varphi_0 = \arctan(y_0/x_0).$$

For the considered example, the obtained dependences r_0 and φ_0 are shown in figure 9.
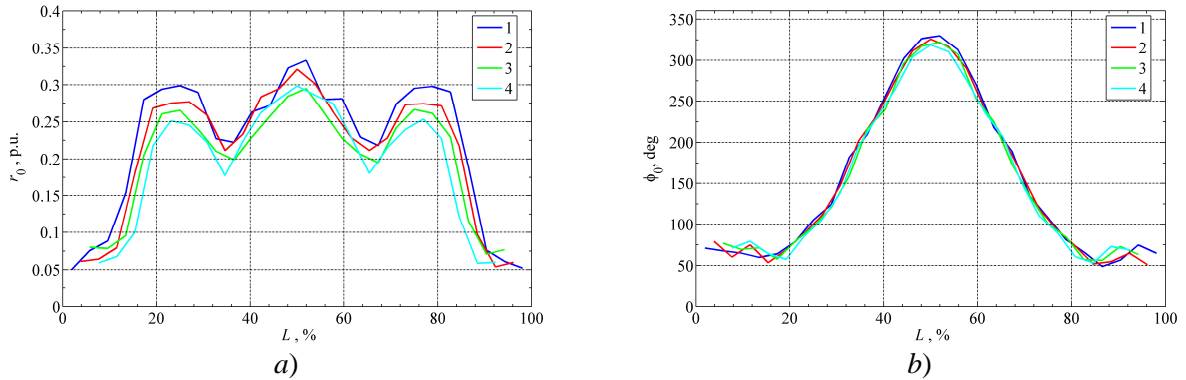

a)

b)

Figure 9 – Dependences of r_0 (*a*) and φ_0 (*b*) in case of short circuit of two (1), four (2), six (3) and eight (4) discs

The dependence of φ_0 versus relative distance L in the range $L = 20 \div 80\%$ can be approximated by the expression

$$\varphi_0 = 130 \sin\left(\frac{3\pi}{100} L - \pi\right) + 190, \tag{2}$$

where φ_0 in degrees.

On the basis of approximation (2) the location of short circuit in the winding can be estimated as

$$L = \arcsin\left(\frac{\varphi_0 - 190}{130}\right) \frac{100}{3\pi}. \tag{3}$$

To use the expression (3) it is necessary to limit the values of φ_0 in the range from 60 to 320° (if $\varphi_0 < 60°$ set to $\varphi_0 = 60°$ and if $\varphi_0 > 320°$ set to $\varphi_0 = 320°$).

Alternative dependence of φ_0 as function of distance L in the range $L = 20 \div 80\%$ can be approximated by the expression

$$\varphi_0 = -8{,}1 \cdot |L - 50| + 330 , \qquad (4)$$

and equation for estimation of L is as follows

$$L = 50 \pm (\varphi_0 - 330)/8{,}1 . \qquad (5)$$

Expressions (4) and (5) are simpler to compute but less accurately describe the dependence of φ_0.

It should be noted that the symmetry of the natural frequencies deviations relatively to the winding middle complicates the task of determining the place of fault. The expression (3) returns the coordinate of L in the range of 20÷50%. To determine which of the two halves of the winding is short-circuited it is necessary to use additional criteria discussed below.

In the range $L = 0 \div 20\%$ and $L = 80 \div 100\%$, the fault location can be approximately determined by the values of r_0 and φ_0 as follows:

- if $r_0 \leq 0{,}12$ the relative distance $L = (0 \div 13)\%$ or $(87 \div 100)\%$; the mean values of the these ranges i.e. $L = 6{,}5\%$ or $L = 93{,}5\%$ can be used for unambiguity;
- if $r_0 > 0{,}12$ and $\varphi_0 < \varphi_{0.L=20\%}$ the relative distance $L = (13 \div 20)\%$ or $(80 \div 87)$; the mean values $L = 13{,}5\%$ and $L = 86{,}5\%$ can be used for unambiguity.

The divergence of results of estimation of the fault location using equations (3) and (5) are shown in figure 9.
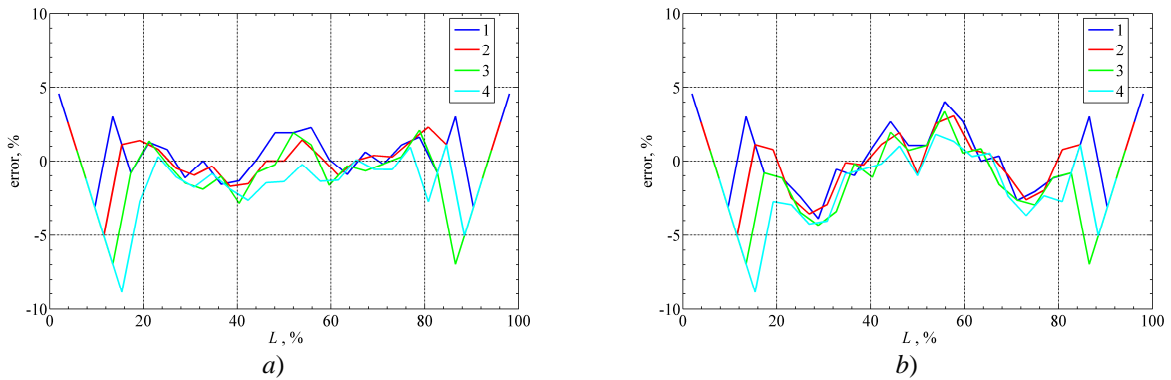

Figure 9 – Divergence of estimation of the fault location in case of short circuit of two (1), four (2), six (3) and eight (4) discs
a) approximation by equation (3); b) approximation by equation (5).

In the range $L = 20 \div 80\%$ the divergence of estimation by equation (3) and (5) and actual position of short circuit does not exceed 5%. In the ranges 0÷20% and 80÷100% divergence of the position estimation does not exceed 5% in case of short circuit of two and four discs. The largest deviation is up to 9% in case of short circuit of eight discs because the discreteness of the position estimation (6,5 and 13,5%).

Table 1 shows the natural frequencies and their deviations in case of short circuit of two turns in discs No. 13, 26 and 39 in model No. 1. The absolute error in this case did not exceed 3%.

The natural frequencies and their deviations in case of short circuit of several discs for model No. 2 are shown in table 2. The divergence of the fault location estimation using the equation (3) for this model does not exceed 5%, and the equation (5) gives error not greater than 7,5% (the latter not shown in table 2).

The radar chart can be divided into 7 regions corresponding to values of L: 0÷13% (87÷100%); 13÷20% (80÷87%); 20÷27% (73÷80%); 27÷33% (67÷73%); 33÷37% (63÷67%); 37÷45% (55÷63%) and 45÷50% (50÷55%). In this case the task of approximate evaluation of the location of the internal short circuit can be done graphically by plotting the triangle of natural frequencies deviation and determination of the region in which is located its centroid of the triangle.

Table 1

Case	Natural frequencies, kHz			Deviations, %			L, %		Error eq. (3), %
	f_1	f_2	f_3	df_1	df_2	df_3	estimated by eq. (3)	actual	
No fault	87	154	211	—	—	—	—	—	—
SC at turns # 1-2, disc # 13	95	155	214	8,8	0,8	1,7	25,8	23,4	2,4
SC at turns # 9-10, disc # 26	87	173	211	0,0	12,2	0,0	50,0	49,9	0,1
SC at turns # 1-2, disc # 39	94	154	217	8,0	0,0	2,9	73,9	73,4	0,6

Table 2

Case	Natural frequencies, kHz			Deviations, %			L, %		Error eq. (3), %
	f_1	f_2	f_3	df_1	df_2	df_3	estimated by eq. (3)	actual	
No fault	160	370	583	—	—	—	—	—	—
SC at discs # 1-8	223	472	752	39,4	27,4	28,8	6,5	7,4	-0,9
SC at discs # 9-22	274	377	615	71,5	1,7	5,3	24,3	27,8	-3,4
SC at discs # 23-24	165	448	718	3,1	20,9	23,0	39,8	42,6	-2,8
SC at discs # 25-30	160	554	587	0,0	49,6	0,6	50,0	50,0	0,0
SC at discs # 31-42	209	423	756	30,8	14,2	29,6	70,3	66,7	3,7
SC at discs # 43-54	253	532	810	58,2	43,7	38,8	93,5	88,9	4,6

Assessment of winding half affected by short-circuit can be done based on the analysis of the amplitudes of the first natural frequencies of frequency responses measured by direct and reverse measurement schemes.

In reference [3] it was shown that in the case where short-circuit takes place close to the winding terminal connected to voltage source, the maximum of spatial voltage distribution for the first natural frequency is higher. This can be explained as follows. When the terminal of winding start is connected to the source and the terminal of winding end is earthed the voltage at the first natural frequency in the first part of the winding, adjacent to winding start, increases to its maximum value, and the voltage at the second part is reduced to zero. This can be explained by the occurrence of a capacitive current in the first part and the inductive current in the second part of the winding.

The occurrence of short-circuit leads to the appearance of the fault current, which tends to compensate the voltage drop across the shorted section of windings. In the discs located near the short-circuited section of the winding, an inductive current caused by inductive coupling induces with opposite direction to the main current flowing from source. Thus, the induced current reduces the voltage growth in the second part of the winding and leads to reduction of maximum voltage achieved as compared with the case of short circuit at first part of winding closer to winding start.

Higher values of voltage to the earth and other windings across the winding under consideration causes a greater capacitive current from this winding. This capacitive current returns to the source through the impedance of the measuring device and leads to increased values of the measured frequency responses, especially at the first natural frequency.

The difference of frequency responses due to the return of a capacitive current is considered in detail in [11].

Unlike external HV winding, where most of the capacitive current returns to the source through the measuring impedance, the internal LV windings may require the use of special measurement schemes with unearthing of source and transformer under measurement [11, 12].

Figure 10 shows the frequency responses for the model No. 2 measured in the direct and reverse schemes, as well as schemes for measurement of diagonal element of transformer admittance matrix (Y_{AA} and Y_{XX}, winding start and end terminals correspondingly) for the cases where the short circuit take place at the first 8 and the last 12 discs.
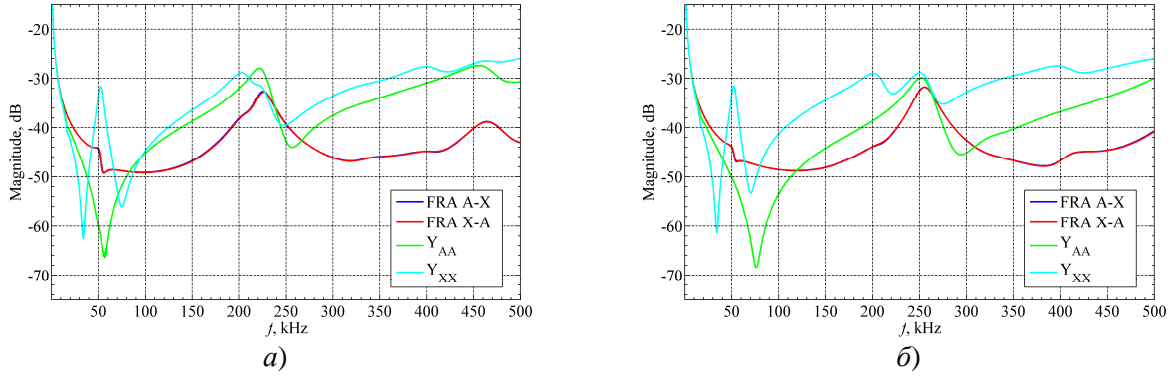
Figure 10 – Frequency responses of winding model No. 2 in case of short circuit at discs # 1–8 (*a*) and discs # 43–54 (*b*)

From figure 10 it is seen that the frequency responses of the direct and reverse schemes coincide with each other in a wide frequency range. It makes impossible to identify which of the two halves of the winding affected by short circuit. However, there are differences in the frequency characteristics Y_{AA} and Y_{XX}.

When short circuit occurs at winding start in the discs with numbers from 1 to 8 the first natural frequency is about 223 kHz. It clearly appears in the frequency characteristics of the FRA and Y_{AA}. Frequency response Y_{XX} in addition to the natural frequencies of the measured winding contains additional resonant peaks. This is due to the fact that during the measurements of winding of the left core leg (see figure 5,b) the end of measured winding (terminal X) were also connected to the end of the winding of the right core leg. Thus, the measured frequency characteristic Y_{XX} contained double resonant peaks represents the result of composition of frequency response of the two windings, in which one has an internal short circuit and shifted natural frequencies, and the second is not affected by short circuit and has no shift of natural frequencies.

In practice, this is a typical situation because the measured winding can be connected in delta or star, and only one phase could be affected by internal fault. As can be seen from figure 10,a the value of the frequency response Y_{XX} at a frequency of 225 kHz is less than value of the frequency response Y_{AA}.

When the fault takes place in the winding end in the coils # 43-54 the overall picture is similar, except that the first natural frequency is about 253 kHz and the value of the frequency response Y_{AA} at this frequency exceeds the value of the frequency response Y_{XX}.

Thus, the half of winding having internal fault can be identified by measurement of diagonal elements of the transformer admittance matrix and the comparison of their values at the first natural frequency.

5. DISCUSSION
A. Applicability of the approach based on the analysis of the natural frequencies
The objectives of this work were to evaluate the possibilities and develop the methodology of FRA interpretation. The proposed approach of FRA interpretation based on the analysis of patterns of natural frequencies deviations gives additional opportunities for the analysis of the results compared using a correlation analysis and integral indexes.

The report shows the possibility of determining the presence of an internal short-circuit fault and an approximate determination of its location in the winding based on deviations of winding natural frequencies. The approach does not claim applicability for all types of windings and types of short circuits. It is an integration of results of the white-box modelling and experimental measurements on models of the windings. The assessment of degree of its applicability for a wide range of practicable types of windings and combinations of internal faults requires further studies.

Concerning the applicability of the natural frequency analysis for the interpretation of other types of winding faults it need to be mention that:
a) Buckling – the radial compression, as a rule, leads to a small reduction of the insulation gap between the core and LV winding or gap between LV and MV windings (in the case of buckling of MV winding in three-winding transformer); this leads to the small decrease of the first natural

frequencies of the considered windings, therefore, it can be identified by the deviation of natural frequencies;

b) Tilting – the deviations of the natural frequencies of the winding are minor; there are changes of amplitude of frequency responses; it can be identified by the absence of significant changes in natural frequency and visible changes of frequency response amplitudes at frequencies corresponding to the winding natural frequencies;

c) Loss of clamping – in general, it may not be accompanied by significant change of axial dimensions and the longitudinal capacitance of the winding; because the electrical length of the winding and its main physical and geometrical parameters remain unchanged, the changes of natural frequencies are negligible; currently the pre-treated pressboard is widely used for spacers having shrinkage at rated clamping pressure of several MPa about few percent; loss of clamping of the order of several tens of percent from its design value, which is typical in operation, may not be identified by analysis of frequency responses and winding natural frequencies; however, obvious changes in natural frequencies may be in case of damage of clamping ring and axial displacement of winding due to high axial short-circuit forces.

B. Sensitivity of the method

Internal short circuit faults, including turn-to-turn faults, cause significant deviations of the natural frequencies. For instance, in the model No. 1 it was found that turn-to-turn short circuit faults in the discs Nos. 13 and 26 lead to changes in the natural frequencies similar to disc-to-disc short circuit faults. Despite a small proportion of the windings affected by the short circuit (0,4 %) the deviations of natural frequencies are about 9-12% (figure 11) in case of turn-to-turn faults. With the increase in the number of turns affected by the short circuit, the deviation of natural frequencies increases almost linearly. The deviations of natural frequencies reach 30-35% when short-circuited section contains 80 turns, which is about 15% of the total number of turns.
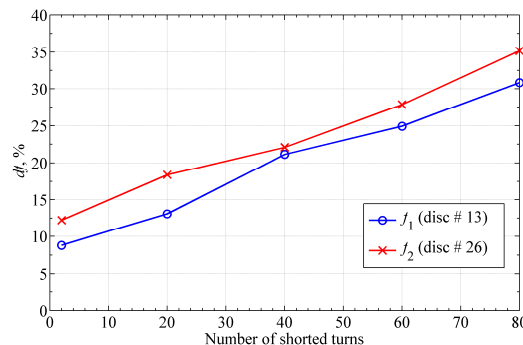

Figure 11 – Deviation of winding natural frequencies depending on number of turns affected by short-circuit fault

Thus, the approach of localization of short circuits based on deviation of the first natural frequencies is quite sensitive both disc-to-disc and turn-to-turn short circuit faults.

C. Accuracy of determining the location of short-circuited section

From figure 3 it is seen that the higher the natural frequency, the greater the degree of variations of the deviations in the ranges of the relative length of the winding $L = 0\div20\%$ and $80\div100\%$. This implies the possibility of increasing the accuracy of the estimation of short circuit place in the start and end parts of the winding by increasing the number of considered natural frequencies.

For instance, in the model No. 1, it was found that when using the first four natural frequencies it is possible to extend the range of application of the approximation φ_0 of the form (2) up to $L = 15 \div 85\%$, and to make the separation in the first (second) part in the ranges $0\div12\%$ and $12\div15\%$ ($85\div88\%$ and $88\div100\%$, respectively). In this case, the largest divergence of the estimation in case of short circuit from 2 to 8 discs is not more than 7%.

In practice, however, natural frequencies with numbers more three are not always clearly expressed in the frequency responses of transformer windings, and there can be difficulties with their identification.

Thus, using the first three natural frequencies is preferred in terms of complexity of computation and the accuracy of fault location.

D. Correction of deviations of natural frequencies
For the studied physical models of disc windings, it was found that the maximum values of the deviations at first natural frequencies differs from each over, as a rule, not more than $1{,}3 \div 1{,}5$ times. For example, the maximum values of the deviations of the first three natural frequencies at figure 3,*a* are about 17, 18 and 15 %. The largest-to-smallest ratio is about 1,2, and this difference can be neglected.

In general case, the maximum deviation of the individual natural frequencies can vary significantly and it is advisable to add into the basic algorithm an adjustment: $df_2' = df_2 k_2$; $df_3' = df_3 k_3$; $df_{base} = \max\left(df_1, df_2 k_2, df_3 k_3\right)$, where k_2 and k_3 – correction factors.

For instance, in the few studied white-box models of disc windings, the greatest deviations along the entire length of the winding at the second and, to a greater extent, the third frequencies were several times smaller than the largest deviation of the first natural frequency. In this case, for a wide range of relative length L the deviation of the first natural frequency df_1 dominates on other natural frequency deviations and without any correction the triangle of deviations at the radar chart is shifted mainly to the first node.

The issue of determining correction coefficients is non-trivial and requires further work. As a first approximation, the correction factors can be defined as $k_i = \left| G_{12.1} / G_{12.i} \right|^{1/i}$, where $G_{12.1}$ and $G_{12.i}$ – the value of the active admittance at the first and i-th natural frequencies. Applicability of this adjustment is based on the results of research on white-box models and physical models of disc windings. As a rule, the greater the deviation of the i-th natural frequency df_i, the greater the maximum of spatial voltage distribution $U_{i.max}$ for this particular frequency (for example, see [3]). In addition, the larger the value of $U_{i.max}$, the greater the currents and the losses, and therefore, the value of the active admittance $G_{12.i}$ at i-th natural frequency. For the first natural frequencies with numbers i and j the ratio of maxima of spatial voltage distribution $U_{i.max}/U_{j.max}$ can be approximately estimated as the ratio of $G_{12.i} / G_{12.j}$ corresponding to open secondary windings.

E. FRA measurement schemes
The approach used in this report to determine natural frequencies is based on comparing the frequency responses of a particular winding with an open and shorted secondary winding.

Measuring the frequency responses with open and shorted low-voltage (or intermediate-voltage) winding is widely used for high-voltage and intermediate-voltage windings.

In case of low-voltage voltage winding connected in star with neutral brought out the common practice is to perform a short circuit by connecting together the phase terminals *a*, *b* and *c* (*u*, *v*, and *w*) without connection to the neutral terminal *n*. This practice is reflected in IEEE Guide for FRA application and interpretation [13].

That is fair enough for the windings connected in delta, where the connection between line terminals of the three phases leads to short circuit each of the phases of this winding. However in case of windings connected in star, this practice is not entirely correct, because instead of short circuiting of winding phase under measurement by means of connection between its start and end points, in fact, the short circuit is done between line terminals of different winding phases. At high frequencies the windings typically have capacitive input impedance, and therefore the connection between line terminals acts like capacitive loading of phase winding under measurement on two other phase windings. Such kind of short circuit has little in common with real short circuiting of phase winding under measurement at high frequency range.

Thus, for identification of winding natural frequencies when secondary windings is connected in star with neutral terminal, the short circuit shall be made by connection together the four terminals *a*, *b*, *c*, and *n* (*u*, *v*, *w* and *n*) or by phase-by-phase short circuits of line and neutral terminals (the latter is more preferable).

To identify the natural frequencies of the inner windings, it is also useful to make the measurement of frequency responses with shorted outer winding (i.e., high-voltage winding), that is not yet a widespread practice.

It should be noted that for a star-connected secondary windings without neutral terminal, the described approach is not applicable in an explicit form, because usually there is no possibility to connect line terminal to the neutral point in case of liquid-immersed transformers. However, given the fact that, in practice, in power transformers the most common winding connection is delta and star with neutral brought out, this approach covers a significant part of mostly used cases.

6. CONCLUSION

The report presents the approach to the analysis of the winding frequency responses based on the determination of natural frequencies of the considered windings and its deviations caused by internal winding faults.

The presence of an internal short circuit in one winding placed on certain magnetic core can be identified by a significant deviation of the frequency of the first antiresonance. The criterion of internal short circuit in the winding could be an increase in the first natural frequencies of the winding. Both disc-to-disc and turn-to-turn short circuit faults cause considerable deviations of winding natural frequencies and thereby it can be detected by FRA.

Depending on location of internal short circuit in the windings there are certain patterns of the deviations of winding natural frequencies which is usually symmetrical with respect to the midpoint of this winding. The presence of patterns allows for localization of internal short circuit in the windings based on the analysis of frequency responses, however, the symmetry of patterns may require the use of additional schemes of frequency response measurement.

The approximate localization of short circuit in the continuous disc winding can be performed graphically by plotting the triangle of deviations of first three natural frequencies and determination of the region in which lies the centroids of this triangle.

The approximate localization of short circuit can also be performed using an approach based on the approximation of the coordinates of the centroids of the triangle of deviations of natural frequencies.

Determination which of the two halves of the windings has a short circuit can be performed by measuring the diagonal elements of the admittance matrix of the considered winding.

For the determination of natural frequencies and interpretation of frequency responses of high-voltage windings the short-circuit of LV winding connected in star with neutral brought out should be done by connection together of three line terminals and neutral terminal or phase-by-phase connections of line terminal of the measured phase with the neutral terminal. Also it is desirable to include into the standard measurement schemes the scheme in which short circuit of outer high-voltage winding is done during the measurement of frequency response of inner low-voltage winding.

ACKNOWLEDGEMENTS

BIBLIOGRAPHY

[1]   M. H. Samimi, S. Tenbohlen, "FRA interpretation using numerical indices: State-of-the-art", International Journal of Electrical Power and Energy Systems, 2017, vol. 89, pp. 115-125.

[2]   DL/T 911–2004 Frequency Response Analysis on Winding Deformation of Power Transformers. The Electric Power Industry Standard of People's Republic of China. 2005.

[3]   A.Yu. Volkov, A.A. Drobyshevski, V.S. Larin, D.A. Matveev, S.A. Drobyshevski. Interpretation of Results of Diagnostics of Power Transformers by Using the Frequency Response Analysis // 46th CIGRE Session, report A2-115, Paris, France, 21-26 August 2016.

[4]   A. Wilk, D. Adamczyk. Investigations on Sensitivity of FRA Method in Diagnosis of Interturn Faults in Transformer Winding // IEEE International Symposium on Industrial Electronics (ISIE), 27-30 June 2011. DOI: 10.1109/ISIE.2011.5984231.

[5] H. Afkar, A. Vahedi. Identifying and Locating Connection Fault of Layer Winding Turn in Distribution Transformer // J. World. Elect. Eng. Tech. 3(2): 74-82, 2014, PP. 74-82.

[6] M. F. M. Yousof, C. Ekanayake, and T. K. Saha. Locating Inter-disc Faults in Transformer Winding Using Frequency Response Analysis // Australasian Universities Power Engineering Conference, AUPEC 2013, Hobart, TAS, Australia, 29 September - 3 October 2013. DOI: 10.1109/AUPEC.2013.6725454.

[7] K. Patel, N. Das, A. Abu-siada and S. Islam. Power Transformer Winding Fault Analysis using Transfer Function // Australasian Universities Power Engineering Conference, AUPEC 2013, Hobart, T AS, Australia, 29 September - 3 October 2013. DOI: 10.1109/AUPEC.2013.6725438.

[8] O. Aljohani, A. Abu-Siada. Application of FRA Polar Plot Technique to Diagnose Internal Faults in Power Transformers // IEEE PES General Meeting, Conference & Exposition, 27-31 July 2014. DOI: 10.1109/PESGM.2014.6939160.

[9] M. Khanali, A.H. Soloot, H.K. Hoidalen, S.H. Jayaram, "Study on locating transformer internal faults using sweep frequency response analysis", Electric Power Systems Research, 2017, vol. 145, pp. 55–62.

[10] V. Larin, D. Matveev, A. Volkov. Study of transient interaction in a system with transformer supplied from network through a cable: assessment of interaction frequencies and resonance evolvement // Proceedings of the 3rd International Colloquium Transformer Research and Asset Management, Split, Croatia, October 15 – 17, 2014.

[11] V.S. Larin, D.A. Matveev. Analysis of transformer frequency response deviations using white-box modelling // CIGRE Study Committee A2 COLLOQUIUM, Cracow, Poland, October 1-6, 2017.

[12] A. Holdyk, B. Gustavsen, I. Arana, and J. Holboell. Wideband Modeling of Power Transformers Using Commercial sFRA Equipment // IEEE Transactions On Power Delivery, Vol. 29, No. 3, June 2014, PP.1446-1553.

[13] IEEE C57.149-2012. IEEE Guide for the Application and Interpretation of Frequency Response Analysis for Oil-Immersed Transformers. ISBN 978-0-7381-8227-8.